ELSEVIER

Journal of Magnetism and Magnetic Materials 159 (1996) L27–L32

journal of magnetism and magnetic materials

Letter to the Editor

On the Barkhausen volume in ultrathin magnetic films with perpendicular anisotropy

A. Kirilyuk *, J. Giergiel, J. Shen, J. Kirschner

Max-Planck Institut für Mikrostrukturphysik, Weinberg 2, D-06120 Halle (Saale), Germany

Received 30 November 1995; revised 6 March 1996

Abstract

Magnetic aftereffect studies as well as in-situ domain observation are performed on γ-Fe/Cu(001) films, providing the Barkhausen volume values for these samples. On the basis of comparative STM studies we propose the structural origin of the Barkhausen volume to be related to the atomic terraces of the Cu(001) substrate.

PACS: 75.60.Ch; 75.60.Ej; 68.55.-a

Keywords: Barkhausen effect; Magnetic domains; Thin film morphology

1. Introduction

The magnetic aftereffect due to thermally activated processes is a general property of all ferromagnetic materials [1]. The key parameter is the Barkhausen volume V_B, which is the elementary magnetization reversal entity. It mainly determines the characteristic reversal time:

$$\tau = \tau_0 \exp\left[\frac{E}{k_B T}\right] = \tau_0 \exp\left[\frac{E_a - 2M_s V_B H}{k_B T}\right], \quad (1)$$

where $\tau_0 \approx$ constant, E_a is the activation energy, M_s is the saturation magnetization, H is the applied magnetic field. The size of the Barkhausen volume also determines the range of magnetic fields where the aftereffect could be observed, and, naturally, the coercive field H_c. If we know the Barkhausen volume in a given sample by origin and size, we may become able to change it at will, thus creating a material fitting particular needs. However, bulk materials are not suitable for such studies for two reasons: on the one hand, the time scale is usually so large that aftereffect can not be observed. On the other hand, it is often difficult to characterize the bulk samples structurally over the scale of 10–100 nm, i.e. the scale responsible for the aftereffect.

By contrast, the magnetic aftereffect is easily observed in ultrathin films [2–5]. At the same time, the preparation of these films may include a well developed structural characterization (e.g. STM imaging). Thus it is much easier to relate the structural and magnetic properties of the sample. From the application point of view, these studies are very important as ultrathin films with perpendicular ani-

* Corresponding author. Present address: EVSF 2, University of Nijmegen, Toernooiveld 1, 6525 ED Nijmegen, The Netherlands. Fax: +31-24-3652190; email: kirilyuk@sci.kun.nl.

PII S0304-8853(96)00303-4

sotropy are promising materials for magneto-optical recording.

γ-Fe/Cu ultrathin films have been extensively studied because of their fascinating magnetic and structural properties [6–10]. They are well known for their extreme sensitivity of atomic scale magnetism upon small structural changes. Magnetic domain pattern has been studied in magnetically virgin Fe/Cu(001) films in Ref. [11]. But, as far as magnetic aftereffects are concerned, we are interested in the relation of macroscopic *magnetization reversal* properties to mesoscopic structural features. Deducing the film morphology from the real-space STM measurements and the Barkhausen volume from the time dependence of the magnetization relaxation, it became possible to correlate the structural and magnetic characteristics. On the basis of our study we propose the common origin of the Barkhausen volume in samples with different morphology to be the atomic terraces of the Cu(001) substrate.

2. Results and discussion

The iron films were deposited in a UHV chamber onto the clean and annealed Cu(001) surface kept at room temperature (RT) or low temperature (LT), 130 K, for comparison. Carbon and oxygen contamination of deposited iron was in the range of 1–2% of a monolayer (ML). Domain images were taken in-situ with the help of a long-distance microscope (the distance between the front of the microscope and the sample was 32 cm, the resolution was better than 10 μm) and a cooled CCD camera. For the illumination, we used linearly polarized light from a discharge lamp and polar-Kerr geometry. Background subtraction was applied to improve the images.

Three samples have been investigated: sample Ia is 3 ML thick RT grown sample; sample Ib is the same as Ia but slightly contaminated by residual gas (20 h at 5×10^{-11} mbar); sample II is 3 ML LT grown sample, and sample III is 7 ML RT grown sample. Recent studies (Refs. [7,8,10], see also our STM pictures below) demonstrate a pronounced difference in the morphology of these samples. The correlation between the film morphology and magnetism of LT grown films has been intensively discussed in Ref. [10].

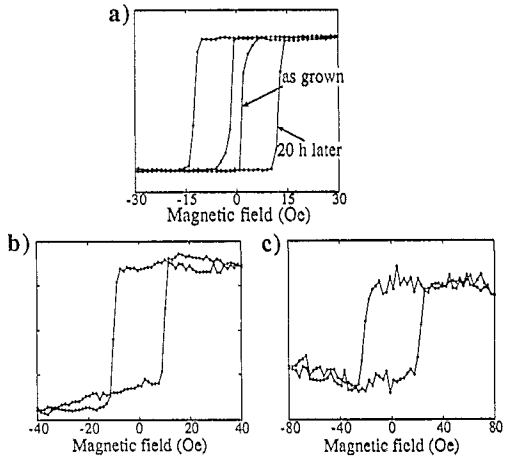

Fig. 1. Kerr ellipticity hysteresis loops for different studied samples; (a) samples Ia,b, (b) sample II, (c) sample III.

Kerr elipticity hysteresis loops (polar geometry) for samples I–III are shown in Fig. 1. It is the sample Ia which can be definitively distinguished from this measurement because of a non-square hysteresis loop indicating a distribution of the coercive fields rather than a single value. The three other samples (Ib, II, III) have quite similar hysteresis loops regardless of slightly different coercive field values.

To observe the magnetic aftereffect, the magnetization relaxation curves were measured for all samples under consideration. The samples are first magnetized to saturation (M_s) in a premagnetizing field of $H_p = 50$ Oe, applied perpendicularly to the film plane. Then the field is reversed (at $t = 5$ s in Fig. 2 to Fig. 5) to a given value $H < H_c$. At $t = 45$ s we saturate the samples to $-M_s$ in order to obtain a reference signal value. Dynamical processes can be analysed from the relaxation of the macroscopic magnetization. In the present work the subsequent change in magnetization is recorded from the variation of the Kerr elipticity. Because all successive in-field magnetic domain patterns may be frozen by switching the field off [4], domain imaging becomes possible in such metastable state. In principle, a particular domain pattern can be associated with any point of experimental relaxation curves.

For the sample Ia, almost no time dependence of the relaxation curves is observed (Fig. 2a). The reversal process is basically field-dependent, i.e. at

the given field value we are able to reverse only some part of the sample area (see Fig. 2a). Other parts stay non-reversed even if one waits much longer time. Large-scale domain imaging reveals a single domain wall travelling across the sample in increasing field (Fig. 2b). Such slight gradient of the coercive field (which may be due to some inhomogeneity of the substrate, e.g. because of a given profile of the sputter gun while cleaning the Cu(001) crystal) is in agreement with the reversal dependencies and together with the large size of the measuring spot (≈ 2 mm) explains the observed shape of the hysteresis.

The time-dependent magnetization reversal, on the contrary, is observed for the sample Ib (see Fig. 3). It appears that the relaxation rate of the magnetization increases rapidly as the absolute value of the field is increased. This strongly suggests (see Refs. [2–4]) that the aftereffect is due to thermal activation of magnetization reversal described by Eq. (1). For the characteristic reversal time, the time $\tau_{1/2}$, for which $M = 0$, is usually considered [2]. Taken from experimental data (i.e. from the curves in Fig. 3a), it provides an estimate of the Barkhausen volume for

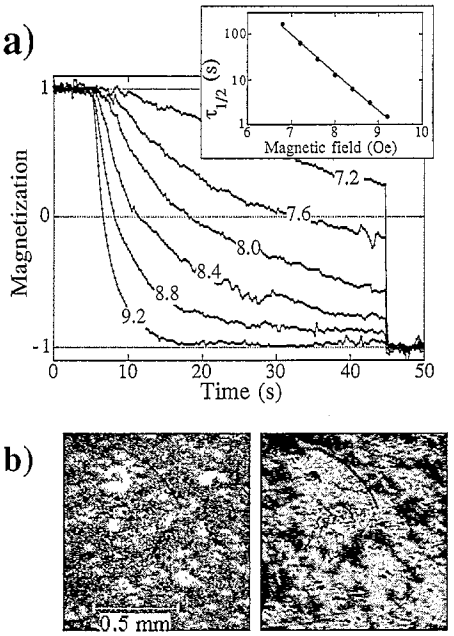

Fig. 3. (a) Magnetization relaxation curves for the sample Ib (sample Ia after being contaminated) at different field values (indicated in the figure in Oe). (b) Domain images of the same location on the sample measured at constant magnetic field 7.6 Oe), but applied over different time (left panel – 20 s, right panel – 60 s).

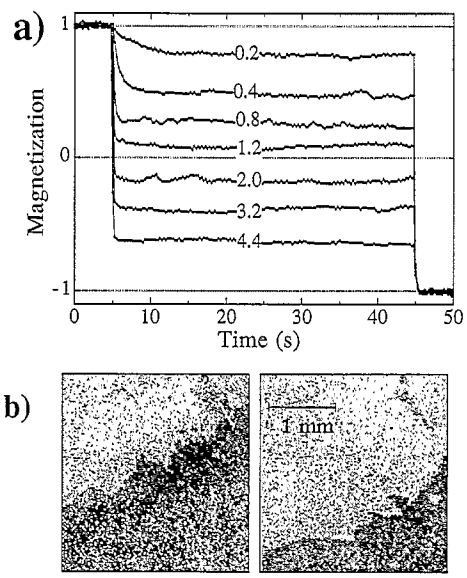

Fig. 2. (a) Magnetization relaxation curves for the sample Ia at different field values (indicated in the figure in Oe). (b) Kerr effect images at two different field values 1.2 Oe (left) and 3.2 Oe (right), showing the movement of the domain wall with increasing field strength.

the given sample. Thus, the slope of the log $\tau_{1/2}(H)$ plot (see inset in Fig. 3a) gives the value of $(2M_sV_B)/(k_BT)$. Assuming the bulk value for M_s, we can estimate V_B. Instead, we will use the 'Barkhausen length' $l_B = \sqrt{V_B/h}$, where h is the Fe thickness. For the sample Ib we thus obtain $l_B \approx 200$ nm.

Of course, this time-dependent behaviour is related to the domain pattern as well (see Fig. 3b). Now the domains are nucleated in many different places, thus their characteristic sizes are becoming smaller. However, the shape of the relaxation curves in Fig. 3a indicates the importance of the domain wall motion process in the magnetization reversal [2,4]. In the opposite case of nucleation dominated process, exponential decay is expected from the very beginning of reversal.

The samples II and III demonstrate a relaxation behaviour very similar to that of the sample Ib (see Fig. 4a and Fig. 5a, respectively). The Barkhausen length of these samples was estimated to be $l_B \approx 220$ nm for the sample II and $l_B \approx 190$ nm for the sample

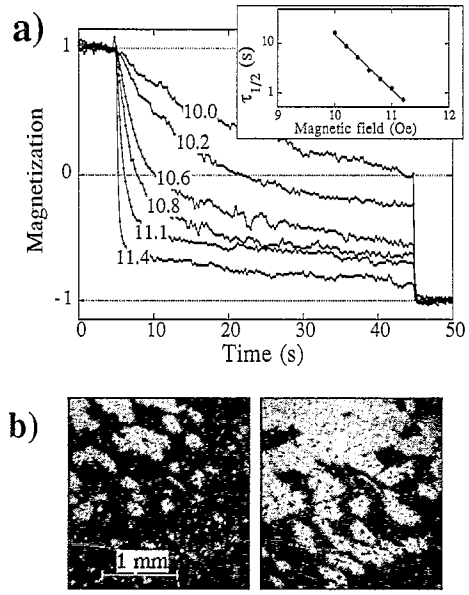

Fig. 4. (a) Magnetization relaxation curves for the sample II at different field values (indicated in the figure in Oe). (b) Domain images of the same location on the sample measured at constant magnetic field (10 Oe), but applied over different time (left panel – 5 s, right panel – 40 s).

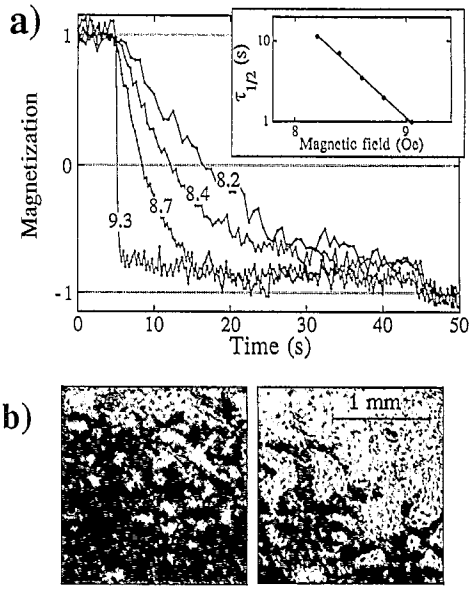

Fig. 5. (a) Magnetization relaxation curves for the sample III at different field values (indicated in the figure in Oe). (b) Domain images of the same location on the sample measured at constant magnetic field (8.2 Oe), but applied over different time (left panel – 5 s, right panel – 20 s).

III in the same way as above (see insets in Fig. 4a and Fig. 5a). Domain imaging reveals qualitatively the same picture for both samples (see Fig. 4b and Fig. 5b), including similar time dependencies.

Table 1 summarises the morphology data, as obtained by STM, and the characteristic 'Barkhausen length' l_B. STM images for our samples as well as for clean Cu(001) substrate are shown in Fig. 6. The images of the samples Ia and Ib were identical; this fact rules out any possible structural changes as a source of the difference in the magnetization reversal behaviour.

Table 1
Structural and magnetic characteristic lengths of the samples

Sample no.	Aftereffect	l_B (nm)	Morphology features
Ia (3 ML, RT)	no		10–20 nm islands
Ib (Ia after 20 h)	yes	200	10–20 nm islands
II (3 ML, LT)	yes	220	3–4 nm 3D islands
III (7 ML, RT)	yes	190	20–40 nm islands + bcc needles
Cu Substrate			200–300 nm atomic terraces

The most straightforward conclusion which follows from Table 1 is that the Barkhausen volume does not depend on the iron film morphology. It is considerably larger than any islands or dislocations observable in the film. However we can compare l_B with atomic terraces on the cleaned and annealed Cu(001) surfaces (see Fig. 6d and Table 1). After sputtering and annealing, we routinely obtain large terraces of 200–300 nm in average, with some of them sized up to 1000 nm. As it is shown by STM, the whole structure keeps distinct traces of these Cu steps even after the iron has been evaporated onto the Cu surface (see STM imges of Ref. [7]). Hence we may tentatively propose a close interconnection between the Cu(001) terraces and the elementary magnetic activation volume. In the thermally activated motion, the domain wall is impeded between successive jumps by some kind of pinning centers, which are therefore responsible for the formation of V_B. Of course, step edges may serve as pinning centers since they represent local zones of enhanced energy density (dipole fields, elastic deformations and stress, enhanced magnetic moments, etc.) This does not mean that the equilibrium domain size

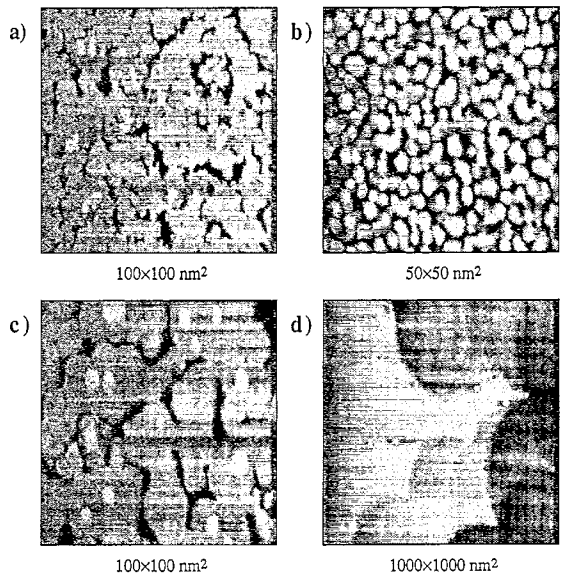

Fig. 6. The surface morphology as measured by STM for different samples: (a) sample Ia (also Ib); (b) sample II; (c) sample III; (d) clean Cu(001) substrate. Scales are indicated on the corresponding images.

should be equal to that of a terrace (Ref. [11] shows contrary), but steps evidently influence the wall *motion* process.

To understand why the domain wall sticks to large Cu terraces but not to smaller iron islands, one should recall the finite domain wall width. Actually the domain wall width should serve as a lower limit of possible Barkhausen length l_B [5]. Unfortunately, no data are available for the domain walls in γ-Fe. Taking into account the standard expression $\delta = \sqrt{A/K}$ (A is the exchange parameter and K is the anisotropy constant), Curie temperature (≈ 300 K) and anisotropy (from Ref. [12]), one can estimate it as $\delta \approx 5$–10 nm. This is obviously much too small to explain our observations. However the Brillouin scattering study in Ref. [12] has been performed for Cu/Fe/Cu(001) sandwiches, and considerable dependence of the anisotropy constant on the Cu coverage thickness suggests an essentially different value for the uncovered iron films. Thus this question remains unsettled.

A further interesting question arises when comparing the behaviour of the samples Ia and Ib. By some reason, the clean as-grown sample Ia does not exhibit the time-dependent aftereffect. Actually this can be explained by ascribing to it a considerably larger Barkhausen volume. Indeed, a large V_B value in Eq. (1) means small reversal field (i.e. H_c, as observed in Fig. 1a) and a very narrow field interval where the aftereffect can be observed over reasonable times. If, in addition, there is an inhomogeneity of the activation energy E_a, it will lead to the inhomogeneity of the reversal field, which is otherwise smeared out by the time-dependent effects.

If we assume the surface contamination from residual gases to concentrate at step edges, which may be justified by occurrence of the barrier at step edges [13], then we may expect pinning centers inhibiting the domain wall motion to aggregate at step edges. This effect leads to subdivision of large Barkhausen volumes into smaller V_B's, corresponding to the Cu(001) terraces. The decrease of V_B leads to the increase of H_c and to the appearance of the observable aftereffect. We have also checked that further surface contamination does not change the V_B any longer. For the samples II and III, in contrary, additional contamination produced no effect on V_B, which can be due to less distorted crystallographic structure of these films [8,10].

3. Conclusion

As a conclusion, the comparative magnetic aftereffect and STM studies strongly suggest the Cu(001) atomic terraces to be the origin for the Barkhausen volume in γ-Fe/Cu(001) films. To explain the vanishingly small interaction of domain walls with iron film morphology features, large domain wall widths have to be assumed.

References

[1] L. Néel, J. Phys. Radium 12 (1951) 339.
[2] M. Labrune, S. Andrieu, F. Rio and P. Bernstein, J. Magn. Magn. Mater. 80 (1989) 211.
[3] G. Bayreuther, P. Bruno, G. Lugert and C. Turtur, Phys. Rev. B 40 (1989) 7399.
[4] J. Pommier, P. Meyer, G. Pénissard, J. Ferré, P. Bruno and D. Renard, Phys. Rev. Lett. 65 (1990) 2054.
[5] A. Kirilyuk, J. Ferré and D. Renard, Europhys. Lett. 24 (1993) 403.

[6] J. Thomassen, F. May, B. Feldmann, M. Wuttig and H. Ibach, Phys. Rev. Lett. 69 (1992) 3831.
[7] J. Giergiel, J. Kirschner, J. Landgraf, J. Shen and J. Woltersdorf, Surf. Sci. 310 (1994) 1.
[8] S. Müller, P. Bayer, C. Reischl, K. Heinz, B. Feldmann, H. Zillgen and M. Wuttig, Phys. Rev. Lett. 74 (1995) 765.
[9] Dongqi Li, M. Freitag, J. Pearson, Z.Q. Qiu and S.D. Bader, Phys. Rev. Lett. 72 (1994) 3112.
[10] J. Giergiel, J. Shen, J. Woltersdorf, A. Kirilyuk and J. Kirschner, Phys. Rev. B 52 (1995) 8528.
[11] R. Allenspach, J. Magn. Magn. Mater. 129 (1994) 160.
[12] J.R. Dutcher, B. Heinrich, J.F. Cochran, D.A. Steigerwald and W. F. Egelhof, Jr., J. Appl. Phys. 63 (1988) 3464.
[13] S. Esch, M. Hohage, Th. Michely and G. Comsa, Phys. Rev. Lett. 72 (1994) 518.